Separation Science and Technology
Publication details, including instructions for authors and subscription information:
http://www.informaworld.com/smpp/title~content=t713708471

Improved Estimation of the Langmuir Adsorption Isotherm Using Multiscale Filtering

Mohamed N. Nounou[a]; Hazem N. Nounou[b]; Ahmed Abdel-Wahab[a]
[a] Chemical Engineering Program, Texas A&M Univsersity at Qatar, Doha, Qatar [b] Electrical Engineering Program, Texas A&M Univsersity at Qatar, Doha, Qatar

To cite this Article Nounou, Mohamed N. , Nounou, Hazem N. and Abdel-Wahab, Ahmed(2009) 'Improved Estimation of the Langmuir Adsorption Isotherm Using Multiscale Filtering', Separation Science and Technology, 44: 11, 2510 — 2525
To link to this Article: DOI: 10.1080/01496390903017352
URL: http://dx.doi.org/10.1080/01496390903017352

Separation Science and Technology, 44: 2510–2525, 2009

ISSN: 0149-6395 print/1520-5754 online
DOI: 10.1080/01496390903017352

Taylor & Francis
Taylor & Francis Group

Improved Estimation of the Langmuir Adsorption Isotherm Using Multiscale Filtering

Mohamed N. Nounou,[1] Hazem N. Nounou,[2] and Ahmed Abdel-Wahab[1]
[1]Chemical Engineering Program, Texas A&M Univsersity at Qatar, Doha, Qatar
[2]Electrical Engineering Program, Texas A&M Univsersity at Qatar, Doha, Qatar

Abstract: Adsorption isotherms play an important role in the design and analysis of adsorption processes. These isotherms are estimated empirically from measurements of adsorption process variables. Unfortunately, these measurements are usually contaminated with errors that degrade the accuracy of estimated isotherms. Therefore, these errors need to be filtered for improved isotherm estimation accuracy. Multiscale wavelet-based filtering has been shown to be a powerful filtering tool. In this work, multiscale filtering is utilized to improve the estimation accuracy of the Langmuir adsorption isotherm in the presence of measurement noise in the data by developing a multiscale isotherm estimation algorithm. The idea behind the algorithm is to use multiscale filtering to filter the data at different scales, use the filtered data from all scales to construct multiple isotherms, and then select among all scales the isotherm that best represent the data based on a cross-validation mean squares error criterion. The developed multiscale isotherm estimation algorithm is shown to outperform the conventional time-domain estimation method through a simulated example.

Keywords: Adsorption, estimation, filtering, Langmuir isotherm, multiscale, wavelets

Received 9 August 2008; accepted 9 March 2009.
Address correspondence to Mohamed N. Nounou, Chemical Engineering Program, Texas A&M Univsersity at Qatar, P.O. Box 23874, Doha, Qatar. Tel.: +974-423-0208; Fax: +974-423-0011. E-mail: mohamed.nounou@qatar.tamu.edu

INTRODUCTION

The presence of toxic heavy metals (such as Lead, Nickel, and Zinc) over the permissible limits in the environment is considered a severe public health problem (1,2). Water containing these metals and their compounds arise from many chemical processes, such as electroplating and inorganic dye manufacturing. Therefore, it is very important to remediate such water from these pollutants before it can be used. Several water purification methods have been utilized, and include chemical precipitation (3) reverse osmosis (4), electro-dialysis, ion exchange, and adsorption, which is the focus of this work.

Adsorption utilizes the capacity of an adsorbent to remove certain substances from a solution. Activated carbon is an adsorbent that is widely used in Water treatment, advanced wastewater treatment, and the treatment of certain organic industrial wastewaters (5,6). Adsorption may be classified as physical adsorption or chemical adsorption. Physical adsorption is primarily due to van der Waals forces and is a reversible occurrence. When the molecular forces of attraction between the solute and the adsorbent are greater than the forces of attraction between the solute and the solvent, the solute will be adsorbed onto the adsorbent surface. An example of physical adsorption is the adsorption by activated carbon. Activated carbon has numerous capillaries within the carbon particles, and the surface available for adsorption includes the surface of the pores in addition to the external surface of the particles. In chemical adsorption, a chemical reaction occurs between the solid and the adsorbed solute, and the reaction is usually irreversible. Chemical adsorption is rarely used in environmental engineering; however, physical adsorption is widely used.

When the adsorbent is placed in a solution containing the contaminant (adsorbate) and the slurry is agitated or mixed to give adequate contact, adsorption of the contaminant occurs. The contaminant concentration in the solution will decrease from an initial concentration, C_o, to an equilibrium value, C_e, if the contact time is sufficient during the slurry test. Usually, equilibrium occurs within about 1 to 4 hours. By employing a series of slurry tests, it is usually possible to obtain a relationship between the equilibrium concentration (C_e) and the amount of organic substance adsorbed per unit mass of the adsorbent (q_e).

The adsorption capacity depends on several factors, such as the adsorbent type, its surface area, and its internal porous structure. Additionally, since the attachment of the pollutant can be physical or chemical, the chemical and physical structures and the electrical charge of the adsorbent can significantly influence the interactions with the adsorbates, and thus the effectiveness of pollutant removal.

Adsorption processes are characterized by their kinetic and equilibrium isotherms. The adsorption isotherms specify the equilibrium surface concentration of the adsorbate as a function of its bulk concentration. Several mathematical models have been proposed to describe the equilibrium isotherms of adsorption. Some of the most popular models include Langmuir, Freundlich, Redlich-Peterson, and Sips. A summary of these isotherms is provided in (7,8). Even though most of these adsorption isotherms are derived based on some theoretical assumptions about the adsorption mechanism, they involve model parameters that need to be estimated from experimental measurements of the process variables. For example, the Langmuir isotherm for single component removal has the following form (9,10):

$$q_e = \frac{Q_c b C_e}{1 + b C_e} \tag{1}$$

where, C_e is the equilibrium liquid phase concentration (mg/l), q_e is the equilibrium solid phase concentration (mg/g), Q_c (mg/g) is the maximum amount of adsorbate per unit weight of the adsorbent to form a complete monolayer, and b (l/mg) is a constant related to the affinity between the adsorbent and adsorbate. In the above Langmuir model, Q_c and b are model parameters to be estimated using the initial concentration and measurements of the equilibrium concentration, C_e.

Unfortunately, measurements of the equilibrium concentration, C_e, are usually contaminated with measurement noise due to random errors, human errors, or malfunctioning sensors. The presence of such measurement noise, especially in large amounts, can degrade the accuracy of the estimated isotherm parameters, which in turn limits the ability of the isotherm to accurately predict the adsorption capacity of the process in which the isotherm is used. Therefore, such noise needs to be filtered for improved estimation of the isotherm parameters.

Noise removal from data is not a simple task since practical measurements are usually multiscale in nature, meaning that they contain features and noise occupying different locations in time and frequency (11). Filtering techniques, however, usually classify noise as high frequency features, and filter the data by removing features with frequency higher than a defined frequency threshold. Since multiscale data may contain correlated noise with low frequency as well as important features with high frequency, noise removal from such data becomes challenging. Thus, multiscale modeling techniques are needed in the estimation of adsorption isotherms to account for this multiscale nature of the data (12).

The objective of this work is to develop a multiscale estimation algorithm that reduces the effect of measurement noise on the accuracy

and prediction of estimated Langmuir isotherm. The rest of this report is organized as follows. In the next Section, time domain estimation of the Langmuir adsorption isotherm is presented. Then, multiscale representation and filtering of data are discussed. Then, the formulation, and algorithm used in multiscale estimation of the Langmuir isotherm are presented, followed by an illustrative example that demonstrates the performance of the developed multiscale Langmuir estimation algorithm. Finally, the paper is concluded with few remarks.

MODEL REPREENTATION AND ESTIMATION OF THE LANGMUIR ISOTHERM

Problem Statement

Given the initial concentration data $\{C_o(1)\ C_o(2)\dots C_o(n)\}$ and measurements of and the equilibrium concentrations, $\{C_e(1)\ C_e(2)\dots C_e(n)\}$, which are assumed to be contaminated with additive zero-mean Gaussian noise, i.e., $C_e = \tilde{C}_e + \varepsilon_e$, where $\varepsilon_e \sim N(0, \sigma^2)$, it is desired to estimate the isotherm parameter, Q_c and b, that satisfy the Langmuir relationship:

$$q_e(k) = \frac{Q_c b C_e(k)}{1 + bC_e(k)},\ k \in [1, n]. \tag{2}$$

Note that the equilibrium uptake, q_e, is not measured and is calculated as follows (13):

$$q_e(k) = \frac{(C_o(k) - C_e(k))V}{w} \tag{3}$$

where, V is the volume of the solution and w is the mass of the adsorbent.

Langmuir Model Representation

The Langmuir isotherm shown in equation (2) is nonlinear and can be linearized as follows,

$$\frac{C_e(k)}{q_e(k)} = \left(\frac{1}{Q_c}\right) C_e(k) + \frac{1}{Q_c b}. \tag{4}$$

Defining: $\alpha_1(k) = C_e(k)/q_e(k)$, $\alpha_2(k) = C_e(k)$, $a_1 = 1/Q_c$, and $a_2 = 1/Q_c b$, the linearized isotherm shown in equation (4) can be written

in matrix form as follows:

$$\underbrace{\begin{bmatrix}\alpha_1(1)\\ \alpha_1(2)\\ .\\ .\\ \alpha_1(n)\end{bmatrix}}_{Y} = \underbrace{\begin{bmatrix}\alpha_2(1) & 1\\ \alpha_2(2) & 1\\ . & .\\ . & .\\ \alpha_2(n) & 1\end{bmatrix}}_{X} \underbrace{\begin{bmatrix}a_1\\ a_2\end{bmatrix}}_{a}. \tag{5}$$

which can be written more compactly as,

$$Y = Xa.$$

Isotherm Estimation Using Least Squares Regression

The linearized model parameter vector, a, can be estimated using Ordinary Least Squares (OLS) regression by solving the following minimization problem (14),

$$\{\hat{a}\} = \arg\min_{a}(Y - Xa)^T(Y - Xa), \tag{6}$$

which has the following closed form solution,

$$\hat{a} = (X^T X)^{-1} X^T Y. \tag{7}$$

Once the parameters a_1 and a_2 are estimated, the original isotherm parameters can be computed as follows:

$$\widehat{Q}_c = 1/\hat{a}_1 \text{ and } \hat{b} = 1/(\widehat{Q}_c \hat{a}_2).$$

It can be seen from equation (6) that the OLS estimation method relies on minimizing the prediction error of the model output, Y, when estimating the isotherm parameters. This is because it assumes that the input matrix, X, is noise-free. However, if the equilibrium concentration data are noisy, then the matrix, X is also noisy, which violates the basic assumption of this approach. Therefore, in the presence of measurement noise in the data, data filtering can improve the estimation accuracy of isotherm parameters. One effective way to do that is through multiscale representation of data, which is presented next.

MULTISCALE REPRESENTATION AND FILTERING OF PROCESS DATA

Multiscale Data Representation

A proper way of analyzing real data requires their representation at multiple scales. This can be achieved by expressing the data as a weighted sum of orthonormal basis functions, which are defined in both time and frequency, such as wavelets. Wavelets are a computationally efficient family of multiscale basis functions. A signal can be represented at multiple resolutions by decomposing the signal on a family of wavelets and scaling functions. The signals in Figs. 1 (b, d, and f) are at increasingly coarser scales compared to the original signal in Fig. 1(a). These scaled signals are determined by projecting the original signal on a set of orthonormal scaling functions of the form (15),

$$\phi_{jk}(t) = \sqrt{2^{-j}}\phi\left(2^{-j}t - k\right), \tag{8}$$

or equivalently by filtering the signal using a low pass filter of length r, $h = [h_1\ h_2 \ldots h_r]$, derived from the scaling functions. On the other hand, the signals in Figs. 1(c, e, and g), which are called the detail signals, capture the differences between any scaled signal and the scaled signal at the finer scale.

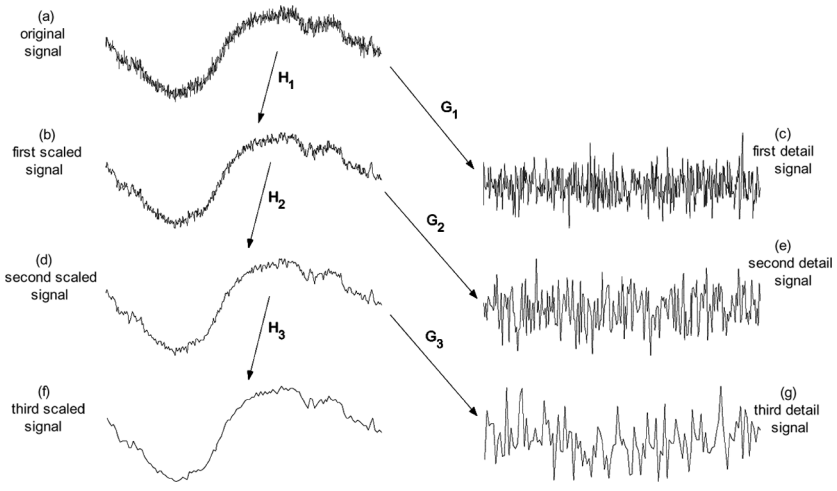

Figure 1. A schematic diagram of data representation at multiple scales.

These detail signals are determined by projecting the signal on a set of wavelet basis functions of the form (15),

$$\psi_{jk}(t) = \sqrt{2^{-j}}\psi\left(2^{-j}t - k\right), \tag{9}$$

or equivalently by filtering the scaled signal at the finer scale using a high pass filter of length r, $g = [g_1\ g_2 \ldots g_r]$, derived from the wavelet basis functions. Therefore, the original signal can be represented as the sum of all detail signals at all scales and the scaled signal at the coarsest scale as follows (15),

$$x(t) = \sum_{k=1}^{n2^{-J}} a_{Jk}\phi_{Jk}(t) + \sum_{j=1}^{J}\sum_{k=1}^{n2^{-j}} d_{jk}\psi_{jk}(t) \tag{10}$$

where, *j, k, J*, and *n* are the dilation parameter, translation parameter, maximum number of scales (or decomposition depth), and the length of the original signal, respectively (16,17).

Fast wavelet transform algorithms of $O(n)$ complexity for a discrete signal of dyadic length have been developed (15). For example, the wavelets and scaling functions coefficients at a particular scale (j), d_j and a_j, can be computed in a compact fashion by multiplying the scaling coefficient vector at the finer scale, a_{j-1}, by the matrices, G_j and H_j, respectively, i.e.,

$$a_j = H_j a_{j-1}, \qquad \text{and} \qquad d_j = G_j a_{j-1},$$

where,

$$H_j = \begin{bmatrix} h_1 & . & h_r & 0 & 0 \\ 0 & h_1 & . & h_r & 0 \\ . & . & . & . & . \\ 0 & 0 & h_1 & . & h_r \end{bmatrix}_{n2^{-j}\times n2^{-j}}, \text{ and}$$

$$G_j = \begin{bmatrix} g_1 & . & g_r & 0 & 0 \\ 0 & g_1 & . & g_r & 0 \\ . & . & . & . & . \\ 0 & 0 & g_1 & . & g_r \end{bmatrix}_{n2^{-j}\times n2^{-j}}. \tag{11}$$

Note that the length of the scaling and detail signals decreases dyadically at coarser resolutions (higher j). In other words, the length of scaled signal at scale (j), is half the length of scaled signal at the finer scale, ($j-1$).

This is due to down-sampling, which is used in discrete wavelet transform. Just as an example to illustrate the multiscale decomposition procedure and to introduce some terminology, consider the following discrete signal, Y_o, of length (n) in the time domain (i.e., $j=0$),

$$Y_o = [y_o(1)\ y_o(2)\ \cdot\ y_o(k)\ \cdot\ y_o(n)]^T, \tag{12}$$

the scaled signal approximation of Y_o at scale (j), which can be written as,

$$Y_j = \left[y_j(1)\ \cdot\ y_j(k)\ \cdot\ y_j(n2^{-j})\right]^T, \tag{13}$$

can be computed as follows,

$$Y_j = H_j Y_{j-1} = H_j H_{j-1} \ldots H_1 Y_o. \tag{14}$$

Note that this decomposition algorithm is batch, i.e., it requires the availability of the entire data set beforehand. An on-line wavelet decomposition algorithm has also been developed and used in data filtering (18).

Multiscale Data Filtering

Multiscale filtering using wavelets is based on the observation that random errors in a signal are present over all wavelet coefficients while deterministic changes get captured in a small number of relatively large coefficients (11, 19–23). Thus, stationary Gaussian noise may be removed by a three step method (19):

1. Transform the noisy signal into the time-frequency domain by decomposing the signal on a selected set of orthonormal wavelet basis functions.
2. Threshold the wavelet coefficients by suppressing coefficients smaller than a selected value.
3. Transform the thresholded coefficients back into the original domain.

Donoho and coworkers have studied the statistical properties of wavelet thresholding and have shown that for a noisy signal of length n, the filtered signal will have an error within $O(\log n)$ of the error between the noise-free signal and the signal filtered with a priori knowledge about the smoothness of the underlying signal (20).

Selecting the proper value of the threshold is a critical step in the rectification process, and several methods have been devised. For good visual quality of the filtered signal, the Visushrink method determines the threshold as (21),

$$t_j = \sigma_j \sqrt{2 \log n} \tag{15}$$

where, n is the signal length and σ_j is the standard deviation of the errors at scale j, which can be estimated from the wavelet coefficients at that scale by

$$\sigma_j = \frac{1}{0.6745} \text{median}\{|d_{jk}|\}. \tag{16}$$

Other methods for determining the threshold are described in (21).

The wavelet coefficients may be thresholded by hard or soft thresholding. Hard thresholding eliminates coefficients smaller than a threshold, whereas soft thresholding also shrinks the larger coefficients towards zero by the value of the threshold. Hard thresholding can lead to better reproduction of peak heights and discontinuities, but at the price of occasional artifacts that can roughen the appearance of the filtered signal, while soft thresholding usually gives better visual filtering quality and fewer artifacts (22). In this work, soft thresholding will be used in filtering adsorption data.

MULTISCALE ESTIMATION OF ADSORPTION ISOTHERMS

Multiscale Formulation of Adsorption Isotherms

The main objective in multiscale isotherm estimation is to reduce the effect of measurement noise in the data on the estimation of isotherm parameters using multiscale filtering. Therefore, the idea is to filter the measured equilibrium concentration data using different decomposition depths, estimate multiple isotherms using the filtered data from these scales, and finally select among all estimated isotherms the one that provides the best prediction.

Denoting the filtered equilibrium concentration data at scale depth (j) as $C_{e,\,j}(k)$, $k \in [1,\, n]$, the isotherm obtained using the filtered data at decomposition scale (j) can be expressed as,

$$q_{e,j}(k) = \frac{Q_{c,j} b_j C_{e,j}(k)}{1 + b_j C_{e,j}(k)} \tag{17}$$

where, the equilibrium uptake can be computed using the equilibrium concentration and the initial concentration as follows,

$$q_{e,j}(k) = \frac{\left(C_o(k) - C_{e,j}(k)\right)V}{w}. \tag{18}$$

Multiscale Isotherm Estimation

The linearized form of the isotherm shown in equation (17) at scale (j) can be written as follows,

$$\frac{C_{e,j}(k)}{q_{e,j}(k)} = \left(\frac{1}{Q_{c,j}}\right) C_{e,j}(k) + \frac{1}{Q_{c,j} b_j}. \tag{19}$$

Defining: $\alpha_{1,j}(k) = C_{e,j}(k)/q_{e,j}(k)$, $\alpha_{2,j}(k) = C_{e,j}(k)$, $a_{1,j} = 1/Q_{c,j}$, and $a_{2,j} = 1/Q_{c,j} b_j$, equation (19) can be expressed in matrix form as,

$$\underbrace{\begin{bmatrix} \alpha_{1,j}(1) \\ \alpha_{1,j}(2) \\ . \\ . \\ \alpha_{1,j}(n) \end{bmatrix}}_{Y_j} = \underbrace{\begin{bmatrix} \alpha_{2,j}(1) & 1 \\ \alpha_{2,j}(2) & 1 \\ . & . \\ . & . \\ \alpha_{2,j}(n) & 1 \end{bmatrix}}_{X_j} \underbrace{\begin{bmatrix} a_{1,j} \\ a_{2,j} \end{bmatrix}}_{a_j}. \tag{20}$$

which can be written more compactly as,

$$Y_j = X_j a_j. \tag{21}$$

The linearized isotherm parameter vector at scale (j), a_j, can be estimated using least squares regression as follows,

$$\hat{a}_j = \left(X_j^T X_j\right)^{-1} X_j^T Y_j. \tag{22}$$

Once the parameters $a_{1,j}$ and $a_{2,j}$ are estimated, the original isotherm parameters can be computed as follows:

$$\widehat{Q}_{c,j} = 1/\hat{a}_{1,j} \tag{23}$$

and,

$$\hat{b}_j = 1/(\widehat{Q}_{c,j}\hat{a}_{2,j}). \tag{24}$$

Multiscale Isotherm Estimation Algorithm

The multiscale isotherm estimation algorithm can be outlined as follows:

1. Filter the measured equilibrium concentration data, C_e, using different decomposition depths (j), $j \in [1, J]$.
2. Using the filtered data from each decomposition depth:
   a. Compute the adsorption uptake using the filtered equilibrium concentration data using equation (18)
   b. Construct a linearized model of the adsorption isotherm as shown in equation (21)
   c. Estimate the linearized model parameters using least squares regression as shown in equation (22)
   d. Compute the original model parameters using the estimated linearized model parameters using equations (23) and (24)
   e. Compute the cross validation mean squares error as follows (21),

$$CVMSE(j) = \frac{1}{n}\sum_{k=1}^{n}\left[\left(C_e^*(k) - \widehat{C}_e(k)\right)^2\right], \tag{25}$$

   where,

$$C_e^*(k) = \frac{1}{2}[C_e(k-1) + C_e(k+1)].$$

3. Select among all scales, the adsorption model with the minimum $CVMSE$ as the optimum isotherm.

ILLUSTRATIVE EXAMPLE

In this section, the performance of the multiscale adsorption estimation algorithm described earlier is illustrated through a simulated example, where $Q_c = 150$ (mg/g), $b = 0.15$ (l/mg). Equations (2) and (3) are used to generate data (assuming $w = 0.1$ g and $V = 0.05\,m^3$), and the data are assumed to be noise-free. Then, the equilibrium concentration data are contaminated with zero mean Gaussian noise. Two different levels of noise are used ($\sigma^2 = 10$ and 20), which correspond to C_e signal-to-noise ratios of 118.5 and 80.0, respectively.

To illustrate the advantages achieved by multiscale filtering, the simulated adsorption data for the case where $\sigma^2 = 20$ are filtered at four scales using the Daubechies-2 filter, and the results are illustrated in Fig. 2. Figure 2 clearly shows the advantages of multiscale filtering, and that the improvement achieved is up to a certain scale above which the filtering accuracy deteriorates.

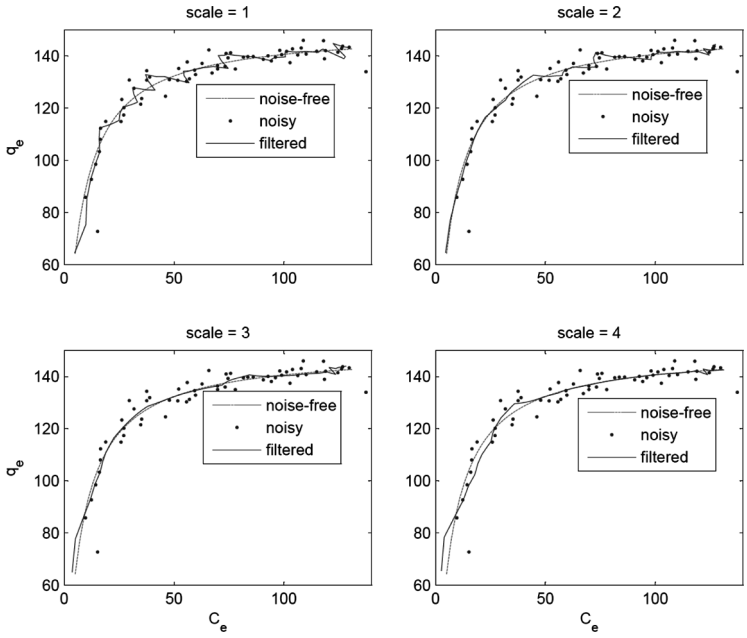

Figure 2. Multiscale filtering of adsorption data at different scales for the case where $\sigma^2 = 20$ [Dotted lines: noise-free, solid lines: filtered, and dots: measurements].

To make statistically valid conclusions about the performances of the time domain method and the multiscale isotherm estimation algorithm, a Monte Carlo simulation of 100 realizations is performed, and the results are presented in Tables 1 and 2.

Table 1 compares the estimated parameters and uptake prediction mean squares errors obtained using the time domain and the multiscale estimation algorithms. These mean squares errors are computed with respect to the noise-free values. Table 1 shows that there is a clear advantage of the multiscale algorithm over the time domain method for both

Table 1. Comparison between the parameter estimation mean square errors (MSE) of the time-domain and multiscale estimation methods

	$\sigma^2 = 10$			$\sigma^2 = 20$		
Estimation method	Q_c *MSE*	$b(10^5)$ *MSE*	q_e *MSE*	Q_c *MSE*	$b(10^4)$ *MSE*	q_e *MSE*
Time-domain	0.50	5.6	16.1	1.34	2.16	41.0
Multiscale	0.38	4.7	4.9	0.83	1.38	8.9

Table 2. Comparison between the parameter estimation mean square errors (MSE) at multiple scales [numbers in parenthesis indicate the percentage each scale is selected as optimum]

	$\sigma^2 = 10$			$\sigma^2 = 20$		
Scale	Q_c *MSE*	$b(10^5)$ *MSE*	q_e *MSE*	Q_c *MSE*	$b(10^5)$ *MSE*	q_e *MSE*
0	0.5	5.6	16.1 (0)	1.34	2.16	41.0 (0)
1	0.38	6.1	6.3 (5)	1.04	1.6	14.5 (7)
2	0.38	4.4	4.6 (95)	0.78	1.35	8.24 (93)
3	0.39	4.8	4.2 (0)	0.98	1.76	7.42 (0)
4	0.43	6.4	6.7 (0)	1.05	1.73	11.74 (0)

the parameters and uptake prediction. Table 2, on the other hand, presents the estimation mean squares errors at various scales also for the isotherm parameters and predicted uptake. Table 2 shows that there is an improvement in the estimation accuracy at coarser scales up to a

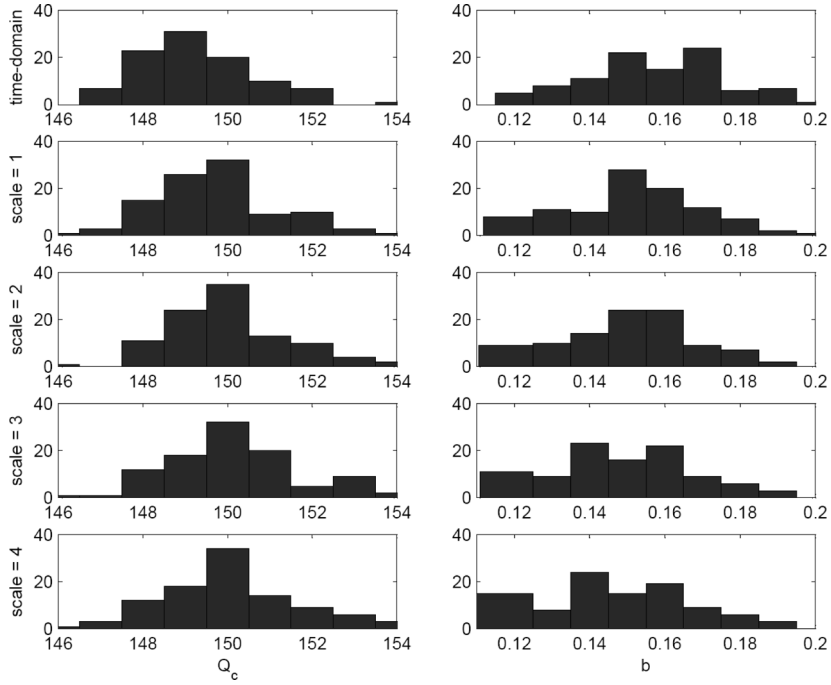

Figure 3. Comparison between the estimated isotherm parameters at multiple scales.

certain scale after which the estimation quality deteriorates. That is why it is important to make a good selection of the estimation scale. Table 2 also lists in parenthesis the percentage each scale is selected as optimum using the cross validation error criterion shown in equation (25). These numbers indicate that reasonable approximation of the optimum scale is achieved by the *CVMSE* criterion.

The improvements in parameter estimation and uptake predictions are also illustrated in Figs. 3 and 4 for the case where $\sigma^2 = 20$. Figure 3 shows histograms of the estimated parameters at different scales, and Fig. 4 shows the predictions of the adsorption uptake at different scales. These figures show the advantages of multiscale estimation of the Langmuir isotherm. For example, in Fig. 3, it can be seen that the histogram of the estimated parameters are more centered around the true value of the parameters at scale 2, which is the optimum scale for model estimation. Also, Fig. 4 shows the advantage of multiscale isotherm estimation even though the predicted uptakes at different scales look similar due to the magnitude of the uptake relative to the prediction errors. The reason behind this improvement (which is shown in Tables 1 and 2 and Figs. 3

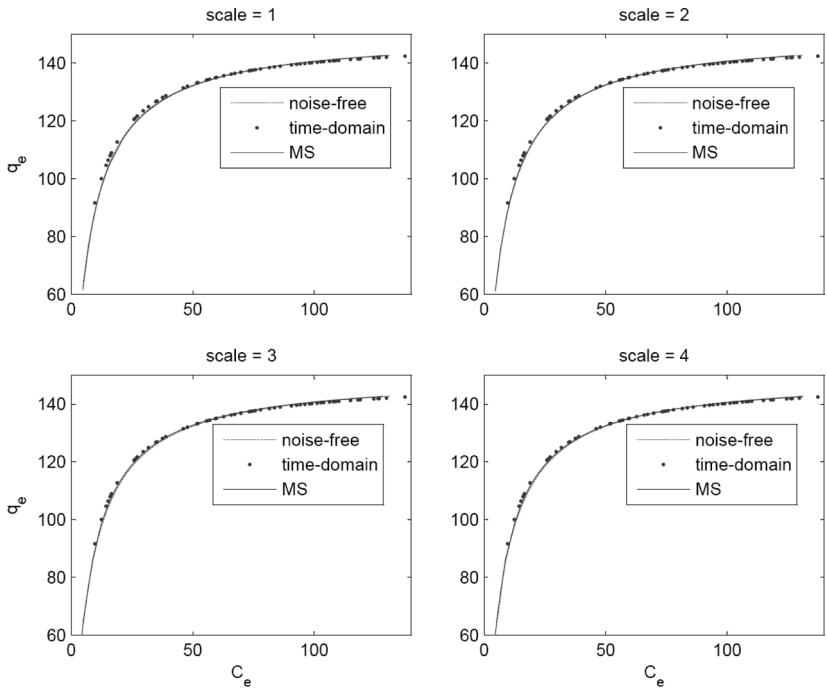

Figure 4. Comparison between the uptake prediction at multiscale and its prediction in the time-domain.

and 4) is due to the noise removal abilities of multiscale filtering, which is illustrated in Fig. 2.

CONCLUSIONS

In this paper, a new multiscale algorithm is developed to improve the estimation and prediction accuracies of the Langmuir adsorption isotherm from noisy measurements. The algorithm relies on denoizing the data using multiscale filtering at different decomposition depths, constructing multiple isotherms at all scales, and then selecting among all scales the optimum Langmuir isotherm based on a cross-validation error criterion. The performance of the developed multiscale estimation algorithm is illustrated through a simulated example that shows its advantages over the time-domain estimation method.

ACKNOWLEDGEMENT

The authors would like to gratefully acknowledge the financial support of Qatar National Research Fund (QNRF).

REFERENCES

1. Bailey, S.; Olin, T.; Brica, R.; Adrian, D. (1999) A review of the potentially low cost sorbents for heavy metals. *Water Res.*, *33* (11): 2469–2479.
2. Naseem, R.; Tahir, S. (2001) Removal of Pb(II) from aqueous/acidic solutions by using bentonite as an adsorbent. *Water Research*, *35* (16): 3982–3986.
3. Henke, K. (1998) Chemistry of heavy metal precipitates resulting from reactions with Thio-Red. *Water Environ. Res.*, *70* (6): 1178–1185.
4. Ning, R. (2002) Arsenic removal by reverse osmosis. *Desalination*, *143* (3): 237–241.
5. Alkan, M.; Doğan, M. (2001) Adsorption of copper(II) onto perlite. *J. Colloid Interface Sci.*, *243*: 280–291.
6. Reynolds, T. D.; Richards, P. (1995) *Unit Operations and Processes in Environmental Engineering,* 2nd Ed.; Thomson-Engineering, Boston, MA.
7. Dabaybeh, M. (2001) *Evaluation of Animal Solid Waster as a new Adsorbent*, M.S. Thesis, Jordan University of Science and Technology.
8. Montgomery, J. (1995) *Water Treatment Principles and Design*, John Wiley and Sons Inc., Hoboken, NJ.
9. Langmuir, I. (1918) The adsorption of gases on plane surfaces of glass, mica, and platinum. *J. Amer. Chem. Soc.*, *40*: 1361–1402.
10. Adamson, A.W. (1967) *Physical Chemistry of Surfaces,* 2nd Ed., Wiley Interscience: New York.

11. Bakshi, B. (1999) Multiscale analysis and modeling using wavelets. *Chemometrics*, *13* (3–4): 415–434.
12. Nounou, M.; Bakshi, B. (2000) Multiscale Methods for Denoising and Compression. In: *Wavelets in Analytical Chemistry*, Walczak, B., ed.; Elsevier: Amsterdam, 119–150.
13. Abdulkarim, M.; Abu Al-Rub, F. (2004) Adsorption of lead ions from aqueous solution onto activated carbon and chemically-modified activated carbon prepared from date pits. *Adsorption Science and Technology*, *22* (2): 119–134.
14. Frank, I.; Friedman, J. (1993) A statistical view of some chemometric regression tools. *Technometrics*, *35* (2): 109–148.
15. Mallat, S. (1989) A theory of multiresolution signal decomposition: the wavelet representation. *IEEE Transactions on Pattern Analysis and Machine Intelligence*, *11* (7): 764.
16. Daubechies, I. (1988) Orthonormal bases for compactly supported wavelets. *Commun, Pure Applied Math.*, *41*: 909.
17. Strang, G. (1989) Wavelets and dilation equations. *SIAM Rev.*, *31*: 613.
18. Nounou, M.; Bakshi, B. (1999) Online multiscale filtering of random and gross errors without process models. *AIChE Journal*, *45* (5): 1041–1058.
19. Donoho, D.; Johnstone, I.; Kerkyacharian, G.; Picard, D. (1995) Wavelet shrinkage: Asymptotia?. *J. Royal Stat. Soc. B*, *57* (2): 301–369.
20. Donoho, D.; Johnstone, I. (1994) *Ideal De-noising in an Orthonormal Basis Chosen from a Library of Bases*, Tech. Report, Dept. of Statistics, Stanford University.
21. Nason, G. (1996) Wavelet shrinkage using cross-validation. *Journal of the Royal Statistical Society*, *58* (2): 463.
22. Coifman, R.; Donoho, D. (1995) Translation-invariant de-noising. Lecture Notes in Statistics, Anestis Antoniadis and Georges Oppenheim, Issue Description: Wavelets and Statistics, New York, 103: 125.
23. Cohen, A.; Daubechies, I.; Pierre, V. (1993) Wavelets on the interval and fast wavelet transforms. *Appl. Comput. Harmonic Analysis*, *1*: 54–81.